Free Radical Intermediates in the Reduction of Quinoxaline *N*-Oxide Antitumor Drugs: Redox and Prototropic Reactions

K. Indira Priyadarsini,*,† Madeleine F. Dennis,‡ Matthew A. Naylor,§ Michael R. L. Stratford,‡ and Peter Wardman‡

Contribution from the Gray Laboratory Cancer Research Trust, Mount Vernon Hospital, P.O. Box 100, Northwood, Middlesex HA6 2JR, U.K., Chemistry Division, Bhabha Atomic Research Centre, Trombay, Mumbai-400085, India, and MRC Radiobiology Unit, Chilton, Didcot, Oxon OX11 ORD, U.K.

Received November 8, 1995⊗

Abstract: The free radical intermediates formed on one-electron reduction of imidazo[1,2-*a*]quinoxaline *N*-oxides RB91724 (**I**), RB90740 (**II**), and RB93918 (**III**) were investigated by pulse radiolysis. Reaction with radiolytically-generated $CO_2^{\bullet-}$ radical anions produced the *N*-oxide radicals. The radicals decayed by second-order kinetics, but the lifetimes of the radicals of **I** increased with increasing pH, whereas the lifetimes of the radicals of **II** and **III** were not significantly affected by pH (pH 4−11). The pK_a values of the protonated radicals were measured as 7.4, 6.2, and 5.5 for **I**, **II**, and **III**, respectively. The radicals reacted with oxygen, with rate constants of 1.6, 3.2, and 1.8×10^8 dm^3 mol^{-1} s^{-1} for **I**, **II**, and **III**, respectively, at pH 7.4. From redox equilibria with viologens and 1-methylnicotinamide, the one-electron reduction potential of **I** was estimated to be −0.70 V, and those for **II** and **III** were estimated as ∼−0.80 V *vs* NHE, i.e., much lower than the corresponding value for the benzotriazine dioxide tirapazamine (−0.45 V). Radicals were also generated by reduction with deoxyribose radicals. Steady-state γ-radiolysis and product analysis indicated a chain mechanism for the reduction of the drugs.

Introduction

Heterocyclic aromatic *N*-oxides are currently being evaluated as hypoxia-selective cytotoxins in the clinical treatment of solid tumors.[1−12] The antitumor selectivity of these drugs is due to both tumor hypoxia and the expression of high levels of reductive enzymes. As the products of reduction of the *N*-oxides are nontoxic, it is believed that intermediate free radicals generated by reduction are involved in the mechanism of cytotoxicity. The principle behind their differential toxicity (oxic *vs* hypoxic cells) is futile "redox cycling", in which the radical is toxic in hypoxic cells but the drug (D) is restored in well-oxygenated tissue by reaction 4:

$$D + e^- \text{ (reductant/enzyme)} + H^+ \rightarrow D^{\bullet-}/DH^{\bullet} \quad (1)$$

$$D^{\bullet-}/DH^{\bullet} + \text{target} \rightarrow DH_2 + \text{damage} \quad (2)$$

$$DH_2 + \text{target} \rightarrow \text{no damage} \quad (3)$$

$$D^{\bullet-} + O_2 \rightarrow D + O_2^{\bullet-} \quad (4)$$

The cytotoxic efficiency of the drug depends on factors such as oxygen tension, redox properties, and kinetics of competing reactions.

Compounds with clinical potential in bioreductive therapy include tirapazamine (SR-4233), 3-amino-1,2,4-benzotriazine 1,4-dioxide.[1,3,7−9] Naylor *et al*. have reported a series of imidazo[1,2-*a*]quinoxaline mono-*N*-oxides that showed selective toxicity toward hypoxic cells.[10−12] They showed DNA damage in experiments where *N*-oxide free radicals were produced. It is hoped that the cytotoxicity might be predicted by understanding the properties of the free radical intermediates. In this study, we investigated the chemical properties of the one-electron-reduced intermediates of three mono-*N*-oxides of this class, RB91724 (**I**), RB90740 (**II**), and RB93918 (**III**), utilizing a one-electron reductant as a model for reductase activity. Depending on the substituent R, they exhibit varying hypoxia-selective toxicity and show selective tumor uptake.[10−12] Thus, **II** is more cytotoxic toward hypoxic cells than **I**, and **III** was synthesized as a more water-soluble analogue of **I**, with the electron-donating alkoxy function possibly counterbalanced by the protonated terminal amine function in the substituent. From their proto-

* To whom correspondence should be addressed.
† Bhabha Atomic Research Centre.
‡ Mount Vernon Hospital.
§ MRC Radiobiology Unit.
⊗ Abstract published in *Advance ACS Abstracts,* May 1, 1996.

(1) Zeman, E. M.; Brown, J. M.; Lemmon, J. J.; Hirst, V. K.; Lee W. *Int. J. Radiat. Oncol. Biol. Phys.* **1986**, *12*, 1239−1242.
(2) Adams, G. E.; Stratford, I. J. *Int. J. Radiat. Oncol. Biol. Phys.* **1994**, *29*, 231−238.
(3) Lloyd, R. V.; Duling, D. R., Rumyantseva, G. V.; Mason R. P.; Bridson, P. K. *Mol. Pharmacol.* **1991**, *40*, 440−444.
(4) Cresteil, T.; Jaiswal A. K. *Biochem. Pharmacol.* **1991,** *42,* 1021−1027.
(5) Edwards, H. S.; Bremner, J. C. M.; Stratford, I. J. *Int. J. Radiat. Biol.* **1991**, *59*, 419−432.
(6) Mason, R. P. *Environ. Health Perspect.* **1990**, *87*, 237−243.
(7) Workman, P.; Stratford, I. J. *Cancer Metastasis Rev.* **1993**, *12*, 73−82.
(8) Zeman,E. M.; Baker M. A.; Lemmon M. J.; Pearson C. I.; Adams J. A.; Brown, J. M.; Lee, W. E., Tracy J. *Int. J. Radiat. Oncol. Biol. Phys.* **1989**, *16*, 977−982.
(9) Minchinton, A. I.; Lemmon , M. J.; Tracy, M. *Int. J. Radiat. Oncol. Biol. Phys.* **1992**, *22*, 701−705.
(10) Naylor, M. A.; Sutton, B. M.; Nolan J.; O'Neill, P.; Fielden, E. M.; Adams, G. E.; Stratford I. J. *Int. J. Radiat. Oncol. Biol. Phys.* **1994**, *29*, 333−337.
(11) Naylor, M. A; Stephens, M. A; Nolan, J.; Sutton, B.; Tocher, J. H.; Fielden, E. M.; Adams G. E.; Stratford, I. J. *Anticancer Drug Des.* **1993**, *8*, 439−461.
(12) Sutton, B. M.; Reeves, N. J.; Naylor, M. A.; Fielden, E. M.; Cole S.; Adams G. E.; Stratford, I. J. *Int. J. Radiat. Oncol. Biol. Phys.* **1994**, *29*, 339−344.

S0002-7863(95)03761-9 CCC: $12.00

tropic, redox, and radical electron-transfer properties, and the results of other radiolysis studies, an attempt has been made to understand drug efficacy.

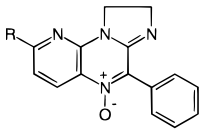

(I) – (III)

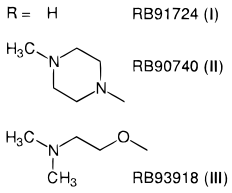

Experimental Procedures

Chemicals. Compounds **I**−**III** were synthesized by the annelation of amidines on haloaromatic compounds.[11] Thus, for **III**, 8-chloro-1,2-dihydro-4-phenylimidazo[1,2-*a*]pyrido[3,2-*e*]pyrazine 5-oxide (1.0 g, 3.35 mmol; synthesized as described previously[11]) was treated with a cold (0 °C) solution of *N*,*N*-dimethylethanolamine (30% sodium salt, 6.1 mL) and the solution allowed to warm to room temperature and stirred for a further 12 h. H_2O (50 mL) was added and the solution extracted with EtOAc (3 × 100 mL), and the combined extracts were evaporated to dryness. The residue was purified by flash chromatography on silica to afford **III** as an orange solid (0.4 g, 34%) after recrystallization from EtOAc/MeOH (mp 158−161 °C); it was characterized by ^{1}H NMR and elemental analysis (C, H, N to ≤±0.4% of theoretical), and the purity (>99%) was confirmed by HPLC. Sodium formate, potassium thiocyanate, and phosphate salts (analytical grade) were obtained from Merck. Deoxyribose, 1-methylnicotinamide (iodide salt), and viologens were from Sigma. All solutions were prepared in water from a "Milli-Q" system (Millipore). Phosphate salts (5 mmol dm^{-3}) were used to adjust the pH with NaOH and $HClO_4$ (Merck). Gases were from British Oxygen Co.

Methods. For the pulse radiolysis experiments, electron pulses (30 ns, 3.5 MeV) from a Van de Graaff accelerator, with typical absorbed doses of 2−3 Gy, were used for most of the studies; to determine rate constants for radical/radical reactions, doses were increased to 15 Gy. The absorbed dose was determined using N_2O-saturated 10 mmol dm^{-3} thiocyanate monitoring $(SCN)_2^{\bullet-}$ at 472 nm.[13] The pulse radiolysis methodology at the Gray Laboratory has been described.[14] All experiments were carried out at room temperature using kinetic absorption spectrophotometry with an optical path of 2 cm.

Radiolysis of water produces three highly reactive species, $H^\bullet$, $^\bullet OH$, and e^-_{aq}, and less reactive molecular species as shown below with the approximate radiation-chemical yields in parentheses (μmol J^{-1}):

$$H_2O \rightarrow e^-_{aq}\ (0.3),\ {}^\bullet OH\ (0.3),\ H^\bullet\ (0.06),\ H_2\ (0.05),\ H_2O_2\ (0.07) \quad (5)$$

In N_2O-saturated solutions, e^-_{aq} is quantitatively converted into $^\bullet OH$:

$$N_2O + e^-_{aq} + H_2O \rightarrow N_2 + {}^\bullet OH + OH^- \quad (6)$$

Both $H^\bullet$ and $^\bullet OH$ were converted to the reductant $CO_2^{\bullet-}$ ($E°(CO_2/CO_2^{\bullet-}) = -1.8$ V *vs* NHE)[15,16] using formate:

$$({}^\bullet OH/H^\bullet) + HCO_2^- \rightarrow H_2O/H_2 + CO_2^{\bullet-} \quad (7)$$

In the presence of 0.1 mol dm^{-3} sodium formate and N_2O, the yield of $CO_2^{\bullet-}$ is 0.68 μmol J^{-1}.[17] In the presence of low concentrations of *N*-oxide drug (D) such that $[HCO_2^-] >> [D]$, $CO_2^{\bullet-}$ was quantitatively converted into drug radicals $D^{\bullet-}/DH^\bullet$:

$$CO_2^{\bullet-} + D/DH^+ \rightarrow CO_2 + D^{\bullet-}/DH^\bullet \quad (8)$$

Table 1. Solvents Used in the HPLC Analyses

drug	aqueous buffer (concn, mmol dm^{-3})	gradient (% organic phase, 3:1 MeCN/H_2O v/v)
I	KH_2PO_4 (40), K_2HPO_4 (10)	15−70% in 7 min
I, **III**	heptanesulfonic acid (5), KH_2PO_4 (10), H_3PO_4 (10)	18−40% in 8 min
II	KH_2PO_4 (40), H_3PO_4 (10)	7−15% in 5 min
III	KH_2PO_4 (10), H_3PO_4 (10)	2−15% in 5 min 4−15% in 5 min

Table 2. Properties of *N*-Oxide Radicals, Reaction Kinetics, and Equilibrium Data

property	RB91724 (**I**)	RB90740 (**II**)	RB93918 (**III**)
pK_a(ground state)	5.6 ± 0.2[a]	5.0 ± 0.1	6.0 ± 0.1
pK_a(radical)	7.4 ± 0.1	6.2 ± 0.1	5.5 ± 0.1
$10^{-8}k_4$[b] (pH 7.4)	1.6 ± 0.1	3.2 ± 0.2	1.8 ± 0.2
$10^{-9}k_8$[b] (pH in parentheses)	4.0 ± 0.2 (5.0) 1.8 ± 0.1 (7.4)	3.0 ± 0.2 (4.2) 1.0 ± 0.1 (7.4)	1.8 ± 0.1 (4.0)
$10^{-8} \times 2k_{10,obs}$[b] (pH in parentheses)	1.0 ± 0.1 (5.4) 0.14 ± 0.01 (7.4) 0.12 ± 0.05 (9)	1.4 ± 0.2 (4.2) 1.5 ± 0.1 (6.2) 1.1 ± 0.3 (8.2)	1.0 ± 0.2 (3.5) 2.0 ± 0.2 (5.5) 1.6 ± 0.1 (7.5)
$10^{-8}k_{11}$[b] (MV^{2+})	3.2 ± 0.1	14 ± 1	6.3 ± 0.6
$10^{-4}k_{-11}$[b] (MV^{2+})	1.8 ± 0.2	nd[c]	0.10 ± 0.01
$10^{-4}K_{11}$ (MV^{2+})	1.8 ± 0.2	nd	63 ± 9
ΔE_{11}(MV^{2+}), V	0.25 ± 0.01	nd	0.34 ± 0.01
$10^{-9}k_{11}$[b] (BV^{2+})	1.3 ± 0.1	1.60 ± 0.04	1.00 ± 0.04
$10^{-5}k_{12}$[b]	nd	6.2 ± 0.4	4.9 ± 0.4
$10^{-9}k_{-12}$[b]	nd	2.8 ± 0.7	1.2 ± 0.2
10^4K_{12}(kinet)[d]	nd	2.2 ± 0.6	4.1 ± 0.8
10^4K_{12}(abs)[e]	nd	2.4 ± 0.8	3.1 ± 1.0
$-\Delta E_{12}$, V	nd	0.22 ± 0.01	0.20 ± 0.02

[a] All uncertainties are sem. [b] dm^3 mol^{-1} s^{-1}. [c] Not determined. [d] Using eq 14. [e] Using eq 13.

Deoxyribose radicals were similarly generated by the reaction of $^\bullet OH/H^\bullet$, assuming a similar radical yield to that of $CO_2^{\bullet-}$.

Steady-state γ-radiolysis experiments of the compounds were carried out in 50 mL syringes using a Co^{60} source, with a dose rate of 1.17 Gy s^{-1} determined by Fricke dosimetry. Analysis by high-performance liquid chromatography (HPLC) utilized a base-deactivated reversed-phase column (Hichrom RPB, 100 × 4.6 mm), with linear gradients of phosphate buffers and 75% acetonitrile (Table 1). The flow rate was 2 mL/min. Detection was by absorbance at 254 nm using either a variable wavelength detector (Waters 486) or a diode array detector (Waters 996). The ion-pairing agent heptanesulfonic acid (sodium salt) was used in some experiments to improve resolution of the radiolysis products.

Results and Discussion

Ground-State Prototropic Equilibria. Ground-state (parent) prototropic equilibria of compounds **I**, **II**, and **III** were determined by following the changes in absorbance with pH at a suitable wavelength (**I**, 390 nm; **II**, 456 nm; **III**, 406 nm); the pK_a values determined are listed in Table 2. Protonation of the *N*-oxide nitrogen is expected to be <1,[18] and these pK_a values may correspond to protonation of one of the ring nitrogens of imidazo[1,2-*a*]quinoxalines. The solutions turned from pale to bright yellow at pH > pK_a.

Absorption Spectra and Decay Kinetics of the Radicals. The transient species formed by one-electron reduction of **I**, **II**, and **III** by $CO_2^{\bullet-}$ were studied by pulse radiolysis of formate/N_2O solutions. In the presence of 50 μmol dm^{-3} **I**, **II**, or **III**, an absorption in the 300−700 nm region was observed, rising in a few microseconds. The bimolecular rate constants for the reduction of these compounds, obtained from the formation kinetics at wavelengths >500 nm over the concentration range 50−100 μmol dm^{-3}, were nearly diffusion controlled, although

(13) Bielski, B. H. J. *Radiat. Phys. Chem.* **1993**, *41*, 527−530.
(14) Candeias, L. P.; Everett, S. A.; Wardman, P. *Free Radical Biol. Med.* **1993**, *15*, 385−394.
(15) Buxton, G. V.; Greenstock, C. L.; Helman, W. P.; Ross A. B. *J. Phys. Chem. Ref. Data* **1988**, *17*, 513−886.
(16) Stanbury, D. M. *Adv. Inorg. Chem.* **1989**, *33*, 69−138.
(17) Mulazzani, Q. G.; D'Angelantonio, M.; Venturi, M.; Hoffman, M. Z.; Rodgers, M. A. J. *J. Phys.Chem.*, **1986**, *90*, 5347−5355.
(18) Perrin, D. D. *Dissociation Constants of Organic Bases in Aqueous Solution*; Butterworths: London, 1965.

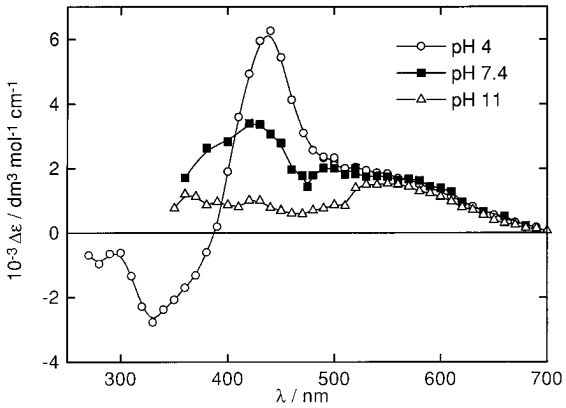

Figure 1. Differential absorption spectra (radical minus the ground state) of the radical anion of RB91724 (**I**) measured by pulse radiolysis (50 μs after the pulse) of N_2O-saturated solutions of **I** (50 μmol dm^{-3}) and sodium formate (0.1 mol dm^{-3}) in phosphate buffer (5 mmol dm^{-3}) at pH 4 (○), pH 7.4 (●), and pH 11 (△).

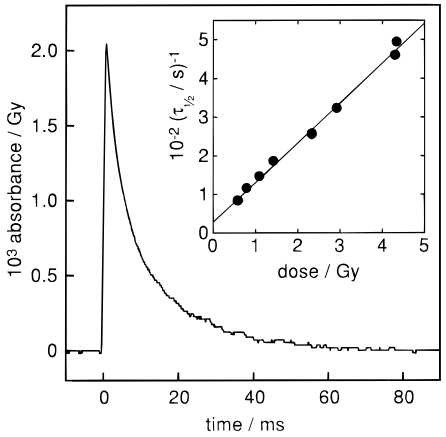

Figure 2. Transient absorption signal at 530 nm observed on reaction of $CO_2^{\bullet-}$ with RB91724 (**I**) at pH 4. The inset shows the variation of the reciprocal of the first half-life of the radical with the pulse dose (radical concentration). Points are averages from two experiments.

they varied slightly with pH; values are listed in Table 2 (k_8). The wavelengths were selected such that there was minimum absorption of the parent, so interference from the bleaching of the parent was negligible.

The absorption spectra of the radicals from reduction of **I**, **II**, and **III** were determined at pH 4, 7.4, and 11 as depicted in Figure 1 for the unsubstituted *N*-oxide **I** (RB91724). The spectrum at pH 4 in Figure 1 shows a maximum at 440 nm and another broad absorption at >500 nm (high ground-state absorptions at low wavelengths make observations difficult). While the absorption at wavelengths <500 nm showed significant change with pH, there was little change at wavelengths >520 nm. The absorption spectroscopy of one-electron reduction of **II** and **III** showed similar spectra, with broad absorption maxima at 520−580 and 480−510 nm for **II** and **III**, respectively (data not shown).

The radicals decayed by second-order kinetics, with first half-lives decreasing with increasing absorbed dose, i.e., with increasing initial radical concentrations. This indicates that the radicals decay predominantly by radical−radical reactions. Figure 2 shows the transient absorption at 530 nm for the radical of **I** at pH 5; the inset shows the linear plot for the reciprocal of the first half-life of the radical with radical concentration. The small intercept (28 ± 7 s^{-1}) indicates an additional first-order process; the slope was used to estimate second-order rate constants. The values thus determined for all the compounds

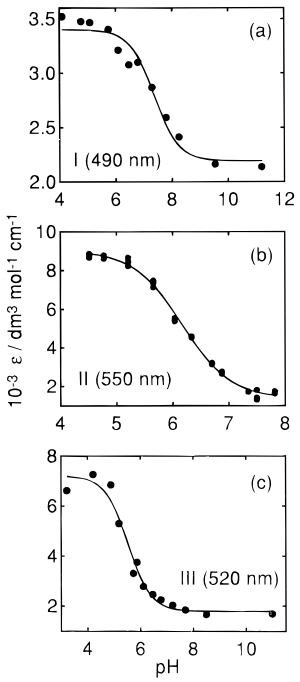

Figure 3. Effect of pH on the extinction coefficient (corrected for ground-state absorption) of the radicals of **I** (a), **II** (b), and **III** (c) measured by pulse radiolysis of N_2O-saturated solution of 50 μmol dm^{-3} drug and 0.1 mol dm^{-3} formate. The lines show the nonlinear least-squares fits to the appropriate function for a prototropic equilibrium.

at various pH conditions are given in Table 2 ($2k_{10,obs}$; see below). In the case of **I**, the radical lifetimes showed significant change with pH, whereas **II** and **III** did not show any marked change in their lifetimes with pH.

Prototropic Equilibria of the Radicals. As the reactivity of radicals is sensitive to pH (see below), a key factor determining the toxicity could be the prototropic equilibria of the radicals:

$$DH^{\bullet} \rightleftharpoons D^{\bullet-} + H^{+} \qquad (9)$$

To determine the pK_a of the one-electron reduced products of **I**, **II**, and **III**, absorption changes were followed at a wavelength where there is significant change with pH in the absorption spectrum of the transient. As the absorption changes in the radicals are maximal at wavelengths where the ground state absorbs (400−500 nm) and there are pK_a values of the parent compounds close to the pK_a values of the radicals, care was taken to minimize errors. The absorption changes were monitored at two different wavelengths, and the ground-state absorbance of each solution was determined at the wavelengths where the transient absorption was monitored. Thus, wavelengths 440 and 490 nm for **I**, 470 and 550 nm for **II**, and 480 and 520 nm for **III** were chosen. Figure 3 shows representative sigmoidal curves for the change in radical extinction coefficients after correcting for the ground-state absorptions. By fitting the curves to the appropriate functions, the pK_a values given in Table 2 were estimated. Whereas the pK_a values for the radicals from **I** and **II** were ∼1−2 units higher than those of the ground states, the pK_a of the radical from **III** was ∼0.5 unit lower than that of the ground state. These pK_a values may reflect protonation of *N*-oxide oxygen in the radical, but the assignments in the ground states are uncertain.

The rate constants for the disproportionation of the radical anion $D^{\bullet-}$ and its protonated conjugate $DH^{\bullet}$ are not necessarily the same. The overall decay of the radicals at any pH (observed

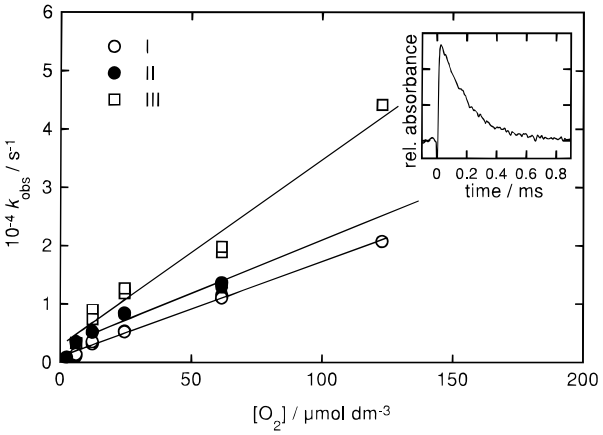

Figure 4. Effect of oxygen on the first-order decay of the radicals of **I**, **II**, and **III** studied by pulse radiolysis of 100 μmol dm^{-3} drug and 0.1 mol dm^{-3} sodium formate solution at pH 7.4, saturated with N_2O and O_2 mixtures (O_2 varied 1−10% v/v): (○) **I**, (●) **II**, (□) **III**. The inset gives the absorption/time plot showing the decay of the radicals of **I** in the presence of 2% oxygen.

rate constant $2k_{10,obs}$ defined by $-d([DH^\bullet] + [D^{\bullet-}])/dt = 2k_{10,obs}([DH^\bullet] + [D^{\bullet-}])^2$) is the result of three reactions:

$$2DH^\bullet \rightarrow DH_2 + D \qquad (10a)$$

$$DH^\bullet + D^{\bullet-}\ (+ H^+) \rightarrow DH_2 + D \qquad (10b)$$

$$2D^{\bullet-}\ (+ 2H^+) \rightarrow DH_2 + D \qquad (10c)$$

The pH variation of the radical decay kinetics reflects these differing reactions, but a full analysis was not attempted. Rate data at different pH values are listed in Table 2.

Reactivity of the Radicals with Oxygen. The effect of oxygen on the radicals formed on one-electron reduction was investigated by following the decay of the drug radical in formate solutions saturated with 1−10% oxygen (v/v), balance nitrous oxide. This corresponds to oxygen concentrations of ∼12−120 μmol dm^{-3}. The decay kinetics were followed at wavelengths >500 nm. Low doses of radiation were used to generate ∼1−2 μmol dm^{-3} radicals, which made the decay from radical−radical reactions slow and resulted in <10% oxygen depletion even at the lowest concentrations. The decay of the radicals of compounds **I**, **II**, and **III** changed significantly in the presence of oxygen at pH 7.4. The radical absorptions decayed exponentially, first-order in [O_2], readily separated from the much slower disproportionation decay. The linear plots indicating the change in observed rate constant for the first-order decay of the drug radical with oxygen concentration are given in Figure 4, and the inset gives an absorption−time plot showing the decay of the radical of **I** in the presence of 2% oxygen. Rate constants k_4 at pH 7.4 were estimated from the slopes of Figure 4 (Table 2). From the radical pK_a (Table 2) it may be observed that the radicals of the three compounds are not in the same form at pH 7.4. Hence, any differences in their rate constants with oxygen may reflect differential reactivity of the protonated and the anionic forms of the drug radicals as well as effects of differences in redox properties.

Estimation of Reduction Potentials. The reduction potentials of the three *N*-oxides were estimated using two redox indicators, viologens[19−23] and 1-methylnicotinamide (MNA),[24−26] and two different approaches.

Reactions with Viologens. Initially we followed electron transfer from drug radical to methyl viologen (MV^{2+}), i.e., the forward reaction in equilibrium 11 representing viologens

$$D^{\bullet-} + V^{2+} \rightleftharpoons D + V^{\bullet+} \qquad (11)$$

generally as V^{2+}. The ratio of the concentration of drug to that of MV^{2+} was ∼10 ([D] ≈ 600−800 μmol dm^{-3} and [MV^{2+}] ≈ 25−100 μmol dm^{-3}). Electron transfer was monitored at 600 nm. Under these conditions, formation of $MV^{\bullet+}$ was observed in a few microseconds, and its rate of formation increased (first order) with increasing concentration of MV^{2+}. Rate constants k_{11} for electron transfer from drug radical to MV^{2+} are given in Table 2. The pH was such that >90% of the drug radical was in the anionic form in these experiments: the reactions were carried out at pH 8.6, 7.8, and 7.0, respectively, for **I**, **II**, and **III**. The radicals of $MV^{\bullet+}$ thus produced decayed completely in a few seconds. We were able to follow independently the reverse process (the reverse reaction in equilibrium 11). To study reaction of methyl viologen radicals ($MV^{\bullet+}$) with the drugs, the ratio of the concentration of MV^{2+} (5 mmol dm^{-3}) to that of drug (100−500 μmol dm^{-3}) was maintained ≥10, and the decay of $MV^{\bullet+}$ was monitored at 600 nm. In the absence of drug, $MV^{\bullet+}$ did not show any decay; however, it decayed slowly (by first-order kinetics) in the presence of **I** or **III**. By following the decay of $MV^{\bullet+}$ as a function of drug concentration, the rate constants k_{-11} for the reaction of $MV^{\bullet+}$ with these compounds were calculated (Table 2). (No significant increase in the rate of decay of $MV^{\bullet+}$ was observed in the presence of **II**.) These rate constants imply that the electron transfer from $MV^{\bullet+}$ to these compounds is not an energetically-favored process, and the reduction potential of $D/D^{\bullet-}$ is significantly more negative than that of $MV^{2+}/MV^{\bullet+}$.

From the above rate constants it appears that it is difficult for the reaction to approach an equilibrium condition. Reaction 11 has much higher rate constants than the reverse (−11), but the former does not interfere significantly in the analysis of the latter. Both reaction 11 and drug radical decay by disproportionation are faster than the reverse reaction (−11) under the conditions used, and hence the latter is rate-determining. These independently-determined forward and reverse rate constants yielded estimates of the equilibrium constant for electron transfer: $K_{11} = k_{11}/k_{-11}$ (Table 2). From these equilibrium constants, and using $E(MV^{2+}/MV^{\bullet+}) = -0.450$ V,[20,23] the reduction potentials $E(D/D^{\bullet-})$ for **I** and **III** were calculated as -0.70 ± 0.01 and -0.79 ± 0.01 V *vs* NHE, respectively.

To test the reliability of these values, we studied the electron-transfer reaction from drug radicals to benzyl viologen (BV^{2+}). As the reduction potential $E(BV^{2+}/BV^{\bullet+})$ is ∼76 mV more positive than that of methyl viologen,[23] one would expect a faster forward reaction (11) with benzyl viologen. The reaction was monitored at 600 nm and the concentration of BV^{2+} varied from 25 to 80 μmol dm^{-3}, keeping the drug concentration constant at 600 μmol dm^{-3}. Near-diffusion-controlled rate constants k_{11} were obtained at pH 7 for the reaction of drug radical with BV^{2+} (Table 2). As expected a very low backward rate constant, $k_{-11} < 1 \times 10^3$ dm^3 mol^{-1} s^{-1}, was observed from $BV^{\bullet+}$ to the drug radicals.

Reactions with 1-Methylnicotinamide. To confirm these reduction potentials, redox equilibria between 1-methylnicoti-

(19) Michaelis, L.; Hill, E. S. *J. Gen. Physiol.* **1933**, *16*, 859−873.
(20) Wardman, P. *J. Phys. Chem. Ref. Data* **1989**, *18*, 1637−1755.
(21) Wold, E.; Kaalhus, O.; Johansen, E. S.; Ekse, A. T. *Int. J. Radiat. Biol.* **1980**, *38*, 599−611.
(22) Watt, G. D.; Burns, A. *Biochem. J.* **1975**, *152*, 33−37.
(23) Wardman, P. *Free Radical Res.Commun.* **1991**, *14*, 57−67.
(24) Anderson, R F.; Patel K. B. *J. Chem. Soc., Faraday Trans. 1* **1984**, *80*, 2693−2702.
(25) Jenson, M. A.; Elving, P. J. *Biochim. Biophys. Acta* **1984**, *764*, 310−315.
(26) Steenken, S.; Telo, J. P.; Novais, H. M.; Candeias, L. P. *J. Am. Chem. Soc.* **1992**, *114*, 4701−4709.

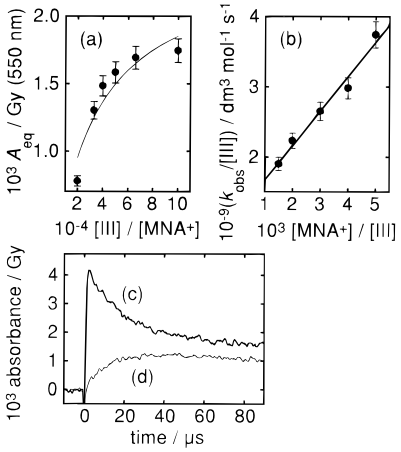

Figure 5. Redox equilibrium between MNA$^\bullet$ and RB93918 **(III)** at pH 8 after a 30 ns pulse. (a) shows the change in absorbance at 550 nm (50 μs after the pulse) with the concentration ratio [**III**]/[MNA$^+$]. The line shows the nonlinear least-squares fit to eq 14. (b) shows the Ratio of k_{obs} for decay at 420 nm divided by [**III**], plotted against the concentration ratio [MNA$^+$]/[**III**]. (c) and (d) give the transient absorptions at 420 and 550 nm, respectively, in a solution containing 40 mmol dm^{-3} MNA$^+$, 20 μmol dm^{-3} **III**, and 1 mol dm^{-3} formate.

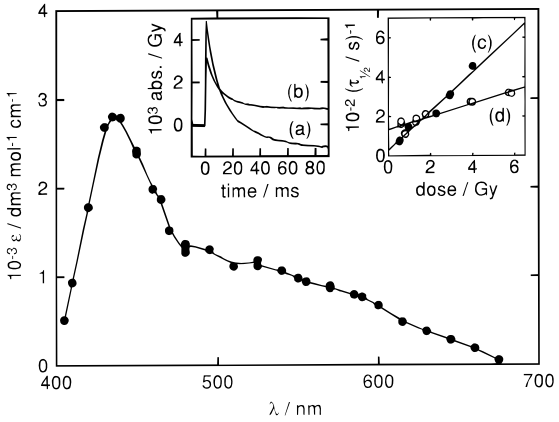

Figure 6. Absorption spectrum of the radicals of **I** generated by reaction of deoxyribose radicals with **I** at pH 4 ([deoxyribose] = 0.05 mol dm^{-3}, [**I**] = 100 μmol dm^{-3}; N_2O). The left inset gives the transient absorptions showing the decay of the radicals of **I** at 450 nm at pH 4 produced on reaction with (a) $CO_2^{\bullet-}$ and (b) deoxyribose radicals. The right inset gives the effects of dose on the reciprocal of the first half-life of **I** observed at 450 nm produced by $CO_2^{\bullet-}$ (c) and deoxyribose radicals (d).

namide (MNA$^+$) and **II** or **III** were studied:

$$D^{\bullet-} + MNA^+ \rightleftharpoons D + MNA^\bullet \qquad (12)$$

Solutions at pH 8 contained 10−50 mmol dm^{-3} MNA$^+$ (iodide salt) and **II** or **III** (10−20 μmol dm^{-3}) with 1 mol dm^{-3} formate. (A high concentration of formate was used to avoid direct reaction of hydroxyl radicals with MNA$^+$.) Under these conditions, MNA$^\bullet$ radicals were initially produced, absorbing at 420 nm, and a reversible electron transfer was observed between these radicals and the drugs in a few microseconds. The observed rate of decay of the radical at 420 nm and the formation of drug radicals at 550 or 580 nm (k_{obs}) was dependent on the concentration of both MNA$^+$ and drug, suggesting reversibility of the reaction. Assuming negligible net radical decay during the equilibrium, a linear relationship is expected:

$$k_{obs}/[D] = k_{-12} + k_{12}([MNA^+]/[D]) \qquad (13)$$

where k_{12} and k_{-12} refer to the forward and reverse reactions in equilibrium 12 and $K_{12} = k_{12}/k_{-12}$.

Equilibrium constants K_{12} were also determined by measuring the changes in absorbances normalized to constant dose at 420 nm and either at 550 nm **(III)** or at 580 nm **(II)**, using eq 14,[20]

$$A_{eq} = [A_{MNA} + K_{12}A_D([D]/[MNA^+])]/[\,1 + K_{12}([D]/[MNA^+])] \qquad (14)$$

where A_D and A_{MNA} are the initial absorbances of the individual radicals and A_{eq} is the absorbance at equilibrium with the mixture. Thus, fitting the measured A_{eq} by nonlinear least-squares to eq 14, K_{12} was determined. Examples of the data, using the kinetic approach and measuring absorbances at equilibrium, for RB93918 (**III**) are shown in Figure 5.

Table 2 lists values of k_{12}, k_{-12}, $K_{12} = k_{12}/k_{-12}$ for **II** and **III** determined using eq 13, and K_{12} measured from changes in absorbance (A_{eq}) and eq 14. The mean values by these two methods are $K_{12} = (2.3 \pm 0.5) \times 10^{-4}$ and $(3.6 \pm 0.6) \times 10^{-4}$ for **II** and **III**, respectively; values of ΔE_{12} are given in Table 2. Using $E(MNA^+/MNA^\bullet) = -1.01 \pm 0.02$ V,[24−26] the reduction potentials $E(D/D^{\bullet-})$ for **II** and **III** were thus estimated as -0.79 ± 0.03 and -0.81 ± 0.03 V, respectively, ignoring the effects of ionic strength (which could be of the same order of magnitude as the uncertainties quoted). The value for **III** is in good agreement with that determined using MV^{2+} as redox indicator.

Reduction by Deoxyribose Radicals. The mechanism of drug radical attack on the biological target (probably DNA[11,28]) is still unclear. One of the hypotheses proposed involves abstraction of hydrogen from a sugar residue of DNA, generating a sugar radical; these radicals are reducing in nature and in turn can reduce another drug molecule, causing a chain reaction.[27] To investigate this hypothesis, we followed the reaction of deoxyribose radicals with the compounds. Deoxyribose radicals were generated by reaction with $^\bullet$OH/H$^\bullet$ radicals in N_2O-saturated solutions at pH 5 (since earlier work had suggested protonated *N*-oxide radicals were more reactive).[27,28] The concentration differentials were adjusted such ([I] = 100 μmol dm^{-3}, [deoxyribose] = 50 mmol dm^{-3}) that direct reaction of $^\bullet$OH with drug was prevented.

The absorption spectrum of the transient from **I** produced by deoxyribose radicals is given in Figure 6. It is similar to that produced by $CO_2^{\bullet-}$ (Figure 1), though its apparent extinction coefficient is almost half. The rate constant for formation of the drug radical by deoxyribose radicals ($(1.3 \pm 0.1) \times 10^8$ dm^3 mol^{-1} s^{-1}) was determined from the first-order buildup of absorption at 450 nm as a function of drug concentration. The apparently smaller value of the extinction coefficient differential (radical minus the ground state, $\sim 2800 \pm 150$ dm^3 mol^{-1} cm^{-1}) compared to $\sim 6200 \pm 200$ dm^3 mol^{-1} cm^{-1} observed with $CO_2^{\bullet-}$ (Figure 1) indicates that not all deoxyribose radicals react with the drug or only about half of them are reducing. (It is difficult to quantify this difference since the ground state absorbs, and correction for the conversion requires a knowledge of the yield. However, at ∼450 nm the ground state of **I** has an extinction coefficient only about 20−25% that of the radical, so the conclusion of a major difference in radical products with the two radicals is clear. This was also confirmed by comparing the yield of $MV^{\bullet+}$ at 600 nm, after reduction of MV^{2+} by $CO_2^{\bullet-}$

(27) Wardman, P.; Dennis, M. F.; Everett S. A.; Patel K. B.; Stratford, M. R. L. In *Free Radicals and Oxidative Stress: Environment, Drugs and Food Additives*; Rice-Evans, C., Halliwell B., Lund, G. G., Eds.; Biochemistry Society Symposium 61; Portland Press: London, 1995; pp 171−194.

(28) Laderoute, K.; Wardman, P.; Rauth, A. M. *Biochem. Pharmacol.* **1988**, *37*, 1487−1495.

or deoxyribose radicals.) Insets a and b of Figure 6 show the absorbance−time plots for the radical of **I** at 450 nm generated from $CO_2^{\bullet-}$ and deoxyribose radicals, respectively. While the former indicates bleaching of the ground state, the latter shows a stable final level, although over the first few milliseconds the decay of the radicals was similar.

To evaluate the decay kinetics of the radicals, we followed the effect of dose on their decay. Insets c and d of Figure 6 show plots of the reciprocal of the first half-life of the transient decay at 450 nm with dose (radical concentration), generated by reaction of **I** with $CO_2^{\bullet-}$ and deoxyribose radicals. There is a larger intercept in the case of reduction by deoxyribose radicals ($\sim$125 s^{-1}) compared to reduction by $CO_2^{\bullet-}$ ($\sim$28 s^{-1}). This suggests that there is a faster first-order process in deoxyribose as compared to formate solutions, possibly due to the abstraction of hydrogen from formate or deoxyribose. Increasing the concentration of deoxyribose increased the intercept, indicating the dependence of the first-order process on deoxyribose concentration. By estimating the first-order components (from the intercepts of 1/half-life *vs* dose plots, as given in inset d of Figure 6 at various concentrations of deoxyribose (0.05−0.5 mol dm^{-3}), an estimate of $(4 \pm 1) \times 10^2$ dm^3 mol^{-1} s^{-1} was made for the hydrogen abstraction reaction from deoxyribose.

The reaction with oxygen of the radical obtained on reduction of **I** by deoxyribose radicals was also studied. The rate constant was found to be comparable (1.5×10^8 dm^3 mol^{-1} s^{-1}) to that obtained (k_4) with drug radicals produced by reduction with $CO_2^{\bullet-}$ at pH 5, suggesting that the nature of the drug radicals is similar with both reductants.

Steady-State γ-Radiolysis and Product Separation. Steady-state irradiation experiments were carried out at a drug concentration of 100 μmol dm^{-3} and with N_2O-saturated 0.1 mol dm^{-3} formate. Loss of parent drug and product formation were monitored using HPLC. Naylor *et al.*[10] studied steady-state radiolysis of **II** at pH 4.8 and 6.9. They observed that the *N*-oxide was reduced to two major products at pH 4.8, identified as a two-electron-reduced product (**IV**) and a dimer (**V**), and

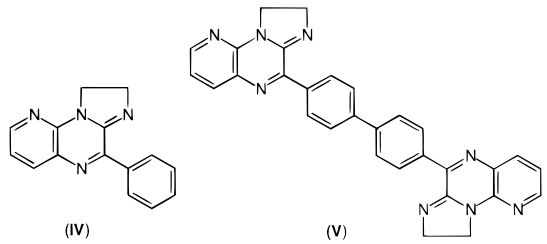

(**IV**) (**V**)

one major product at pH 6.9, the two-electron-reduced species. In our study we also observed two products with compounds **I** and **III** at pH 4 and one major product at higher pH. Compound **II** appeared unstable at pH 4 and yielded three peaks in addition to the parent prior to irradiation, all of which increased with radiation. Figure 7 gives HPLC chromatograms for the reduction of **I**, and the product distribution at pH 5 and 10.6.

Disproportionation of the radical anion could produce the two-electron-reduced species and radical−radical recombination accounts for dimer formation. The detailed mechanism for the formation of these products from the *N*-oxide radicals was described previously.[10] Production of **IV** and **V** involves loss of two radicals and the loss of one or two drug molecules, respectively. Figure 8 shows the variation in the loss of drug **I** with the radical input at pH 4, 7.4, and 11 (the pK_a of the radical is 7.4). At pH 4, about two drug molecules are reduced for the input of one radical, suggesting a chain mechanism for the reduction of **I** similar to that observed in the case of di-*N*-oxides like tirapazamine.[27,28,30] If there is no chain reaction,

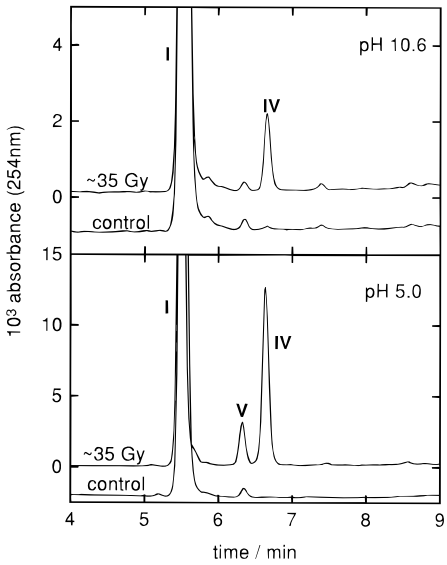

Figure 7. HPLC chromatograms of an irradiated solution of **I** (100 μmol dm^{-3}) and 0.1 mol dm^{-3} deoxyribose/N_2O at pH 10.6 or 5.0.

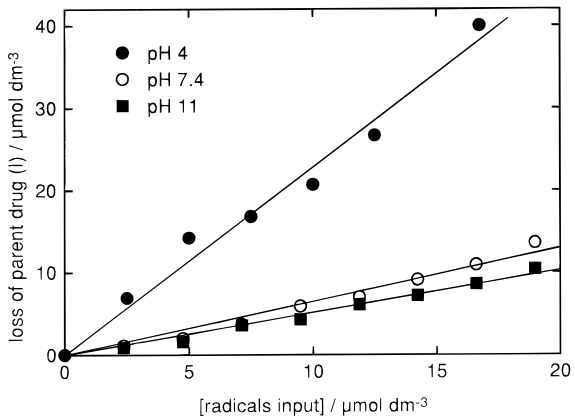

Figure 8. Loss of the parent drug (**I**) at various pH plotted against the radical concentration input after irradiating a solution of **I** (100 μmol dm^{-3}), formate (0.1 mol dm^{-3}), and N_2O at pH 4 (●), 7.4 (○) or 11 (■).

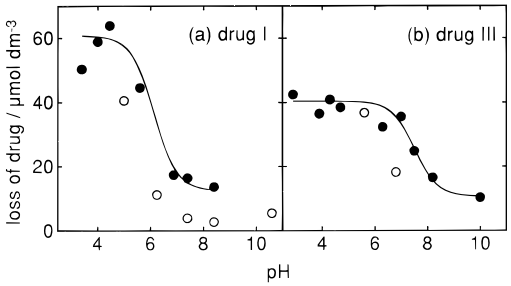

Figure 9. Effect of pH on the loss of the parent drug (a) **I** or (b) **III** on reaction with formate radicals (●) or deoxyribose radicals (○) (initial concentration of **I** or **III** $\sim$100 μmol dm^{-3}, dose $\sim$34 Gy).

one might expect 0.5 drug molecule to be reduced for one radical produced. The chain length of such a process is defined as the number of drug molecules lost for the input of two radicals. Thus, chain lengths of 4, 1.5, and 1.0 were obtained for the reduction of **I** at pH 4, 7.4, and 11, respectively. Similar studies with **III** indicated chain lengths of 4, 2.9, and 1.3 at pH 4, 7.4, and 11, respectively. The chain lengths at physiological pH (pH 7.4) for all three drugs were calculated to be 1.5, $\leq$2,[12] and 2.9, respectively, for **I**, **II**, and **III**. Figure 9 shows loss of the drug molecules of **I** and **III** with pH at an absorbed dose of 34 Gy. From these figures, apparent "pK_a" values could be

estimated from the inflection points as 6.3 and 7.3, respectively, for **I** and **III**. These values are almost 1−2 units higher than the pK_a values estimated by pulse radiolysis from the radical absorptions (Table 2). While the pH profiles suggest the protonated radicals are more efficient hydrogen abstractors, clearly other reactions are occurring with a differing pH dependence.

Steady-state radiolysis studies of **I** and **III** were also carried out using 0.1 mol dm^{-3} deoxyribose instead of formate, keeping all other conditions the same. The loss of the parent and the formation of products were monitored by HPLC. Product distributions similar to those obtained with formate were observed, and loss of the parent was followed at different pH values. The results are included in Figure 9. From pulse radiolysis studies, we observed that only about half the initial radicals of deoxyribose appear to form drug radical anions; hence, the loss of the drug at a given dose is also expected to be about half. Irradiation in the presence of O_2/N_2O (20/80 v/v) and formate did not cause any degradation of the drug, and no product could be observed, confirming that the parent is restored by protective electron transfer to oxygen.

Conclusions

Free radical intermediates involved in the bioreductive activation of three *N*-oxides, RB91724 (**I**), RB90740 (**II**), and RB93918 (**III**), have been investigated in model systems using radiolysis methods. The prototropic and redox properties of the radicals were quantified. The radicals have natural lifetimes of a few milliseconds (at micromolar concentrations) in the absence of oxygen but could be much longer at the low steady-state concentrations likely in cellular systems. In the case of the prototype imidazo[1,2-*a*]quinoxaline *N*-oxide, RB91724, the pK_a was shown to be around physiological pH and changed significantly by substituents.

A critical step in bioreductive activation is transfer of a single electron to form the drug radical anion. The rates of such electron-transfer reactions are dependent on the energetics of the reaction, reflected in the reduction potentials of the couples involved. The reduction potentials of the mono-*N*-oxides were estimated to be −0.7 to −0.8 V *vs* NHE. The resonance stability of the radical over the extended conjugated system might be expected to increase the electron affinity of the drugs. However, they are less electron-affinic than most nitroarenes and benzotriazine di-*N*-oxides.[29,30] The reduction potential of the benzotriazine di-*N*-oxide tirapazamine has recently been estimated as −0.45 V.[31] This is reflected in the high reactivity of the radicals of **I**, **II**, and **III** with oxygen (rate constant $k_4 \approx 2 \times 10^8$ dm^3 mol^{-1} s^{-1}). The radicals of these mono-*N*-oxides are therefore ∼20−40 times more reactive toward oxygen than the radicals of nitro compounds or di-*N*-oxides such as tirapazamine.[27,28] Too high a rate constant could prevent radioresistant hypoxic cells from being killed by the cytotoxin, except in extreme hypoxia, thus accounting for poor *in vivo* activity of drugs of this type despite potent tumor cell killing under anoxia *in vitro*.[32]

The *N*-oxides **I**−**III** have one-electron reduction potentials (drug/radical couple) around 0.3 V lower than many nitroarene bioreductive drugs or tirapazamine.[20,31] In view of the reported relationships between rates of drug reduction (by reduced flavins or typical one-electron reductases),[27] it might have been expected that these *N*-oxides would be reduced by anoxic cells at least 2 orders of magnitude slower than nitroarenes or tirapazamine. In view of the reported biological activities,[10−12] this prediction from earlier experience is clearly in doubt. This points to the need for further work in correlating chemical properties with rates of biological activation.

Deoxyribose radicals react with the drug, at a rate an order of magnitude less than the diffusion-controlled limit; with RB91724 (**I**) and RB93918 (**III**) only half the initial radicals appear to result in reduction. Steady-state radiolytic reduction of the *N*-oxides in the presence of 0.1 mol dm^{-3} formate as hydrogen donor leads to the formation of two products at low pH (pH ≈ 4) and one product at pH > 7. The loss of drug indicates a chain mechanism. A similar product distribution was observed by initiating the reduction with deoxyribose radicals, suggesting a more efficient hydrogen abstraction process compared to that of formate. Loss of the chain process at pH > 7 suggests that the protonated radical is more important in initiating the chain reaction than its conjugate. A radiolytic chain reaction may model a mechanism for clustered damage on DNA. The efficiency of drug reduction in cellular systems is thus a result of many factors, including the lifetimes of the radical, reduction potential, reactivity with traces of oxygen, and ability to abstract hydrogen (e.g., from a sugar residue of DNA). The latter property seems to be associated with the prototropic equilbria of the radicals; the radical pK_a defining such equilibria is both amenable to controlled manipulation and linked to reduction potential.

Acknowledgment. The authors are grateful to Drs. S. A. Everett, L. P. Candeias, and I. J. Stratford for helpful discussions, Mr. K. B. Patel for expert assistance with steady-state radiolysis experiments, and Dr. B. Vojnovic and his team for the continuous development of the pulse radiolysis equipment. K.I.P. thanks the Department of Science and Technology, Government of India, and Commission of the European Communities for the "Marie Curie" Research Fellowship. This work was also supported by the Cancer Research Campaign (CRC) and the Medical Research Council.

JA953761O

(29) Wardman, P. *Environ. Health Perspect.* **1990**, *87*, 237−243.
(30) Wardman, P.; Priyadarsini, K. I.; Dennis, M. F.; Everett S. A.; Naylor, M. A.; Patel K. B.; Stratford, I. J.; Stratford, M. R. L.; Tracy, M. *Br. J. Cancer* **1996**, *73* (Suppl. XXVII), in press.
(31) Priyadarsini, K. I.; Tracy, M.; Wardman, P. *Free Radical Res.*, in press.
(32) Naylor, M. A. *Oncol. Res.* **1994**, *6*, 483−490.